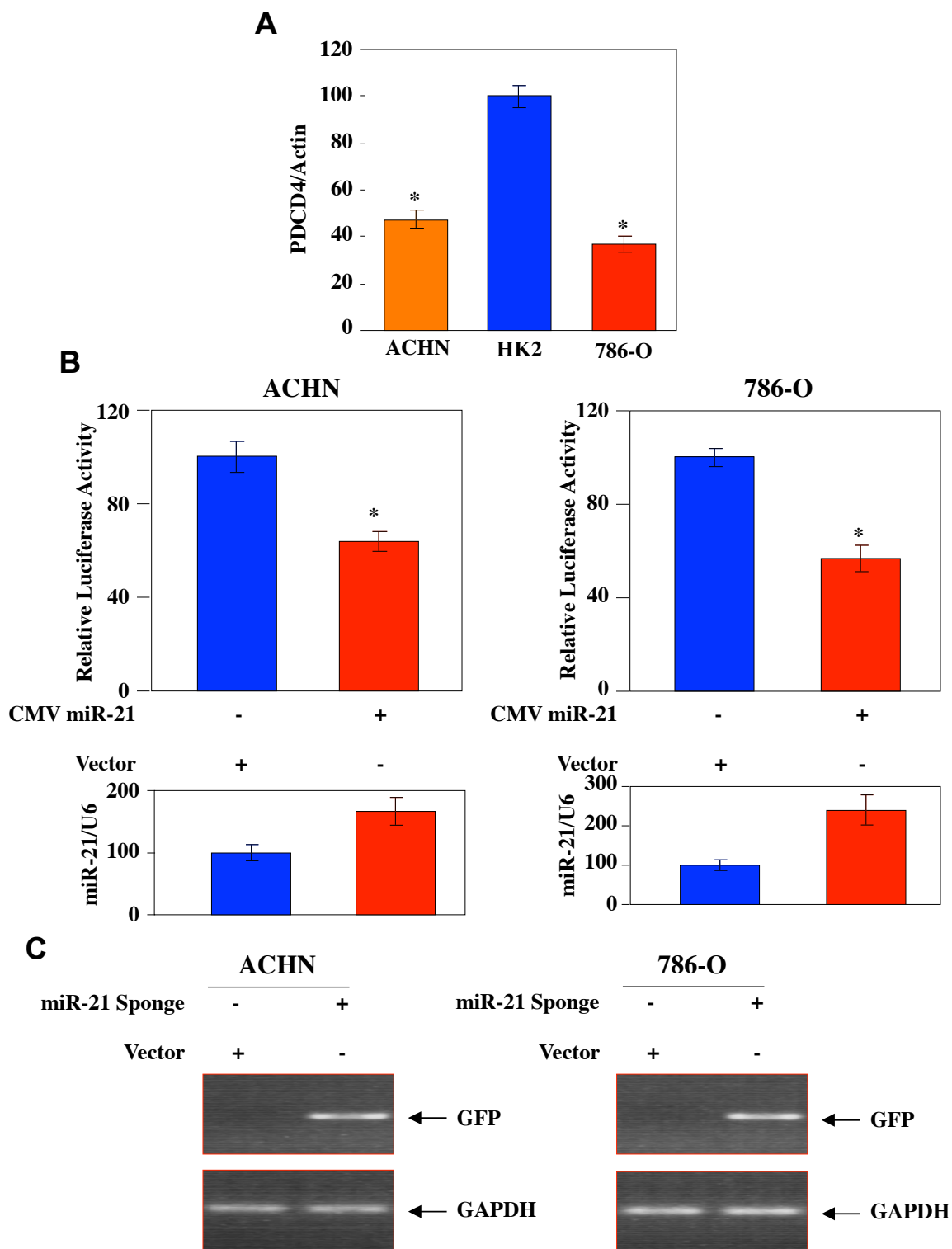
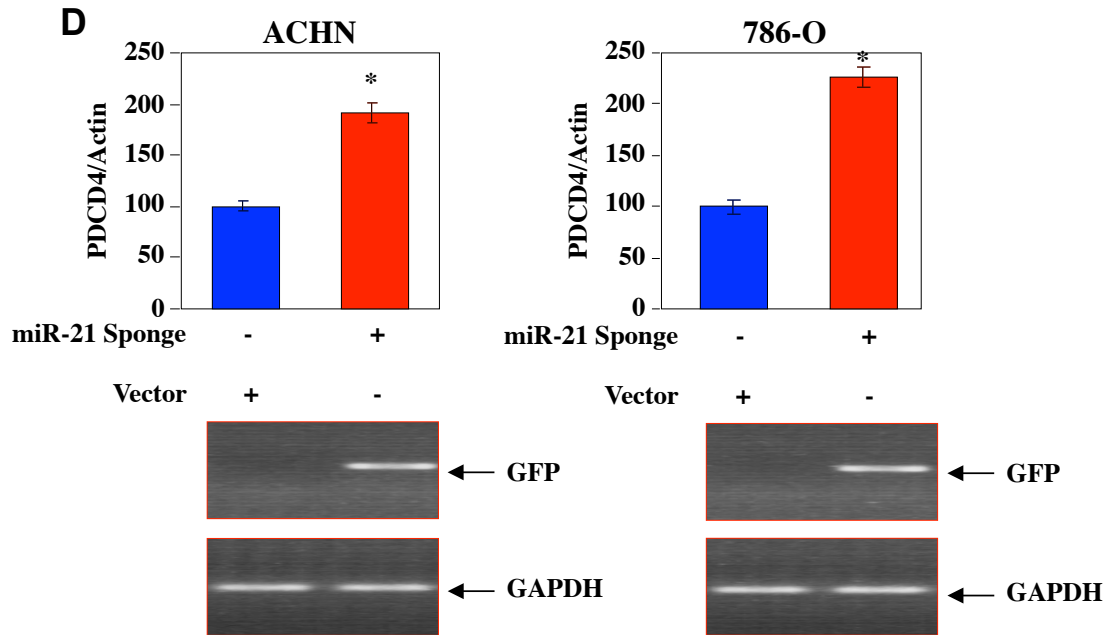


Supplementary Table 1

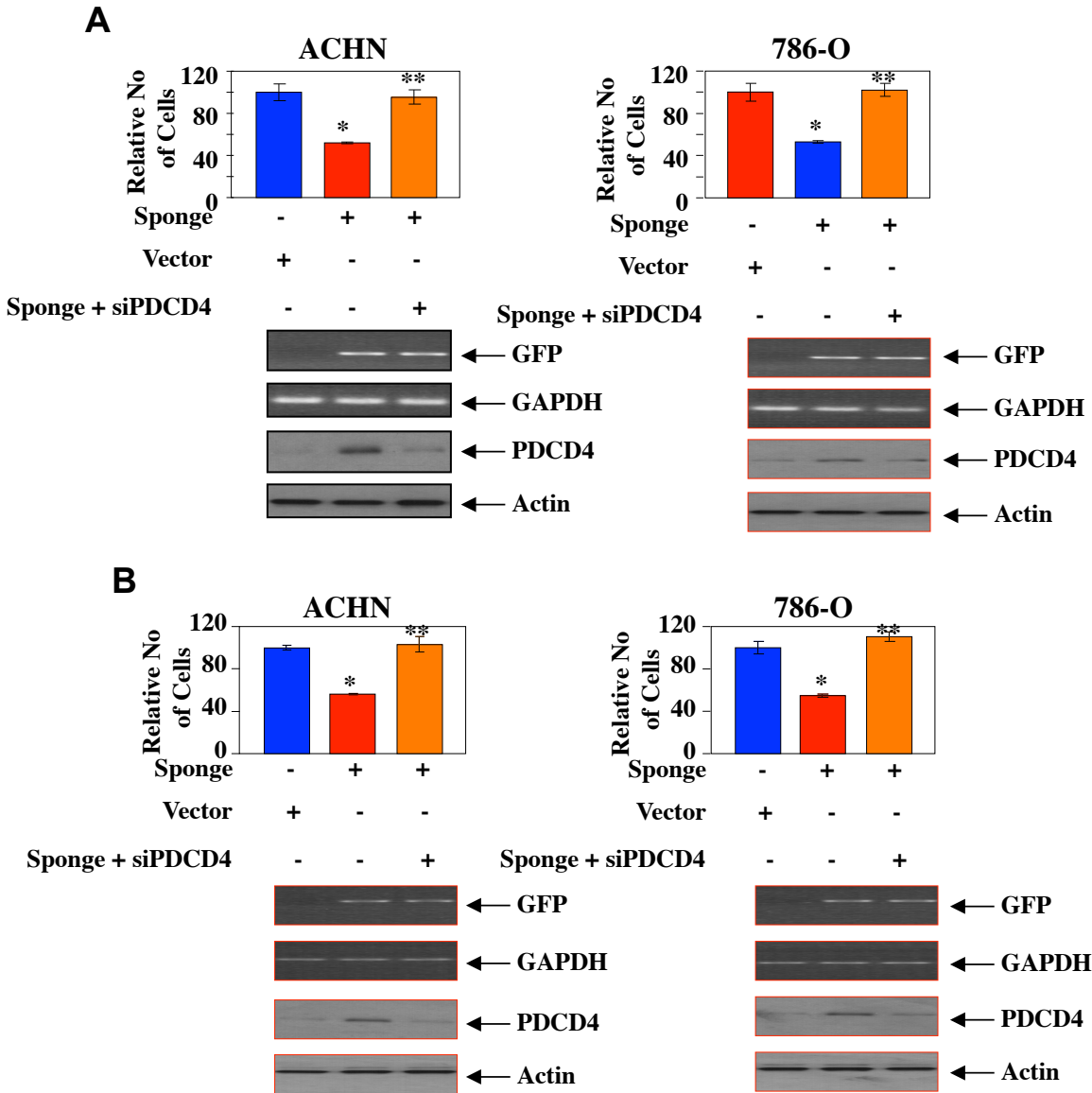
<b>Antigen</b>	<b>Species</b>	<b>Vendor</b>	<b>Cat. No</b>
PDCD4	goat polyclonal	Santa Cruz Biotechnology	Sc-27123
p65	goat polyclonal		Sc-109-G
I $\kappa$ B- $\alpha$	rabbit polyclonal		Sc-371
Myc	mouse monoclonal		Sc-40
IgG	mouse monoclonal	Santa Cruz Biotechnology	Sc-69786
phospho-S6 kinase ( Thr-389)	rabbit polyclonal	Cell Signaling Technologies	9205
S6 kinase	rabbit polyclonal		9202
phospho-IKK ( Ser-180/181)	rabbit polyclonal		2681
IKK $\beta$	rabbit polyclonal		2684
Phosphor-Akt ( Ser-473)	rabbit polyclonal		9271
Phosphor-I $\kappa$ B- $\alpha$ (Ser-32)	rabbit polyclonal		9241
Akt	rabbit polyclonal		9272
Phosphor-p65 (Ser-536)	rabbit monoclonal		3031
Rictor	rabbit polyclonal		2140
Actin	rabbit polyclonal		Sigma
FLAG	mouse monoclonal	F-4042	
HA	mouse monoclonal	Covance	MMS-101P



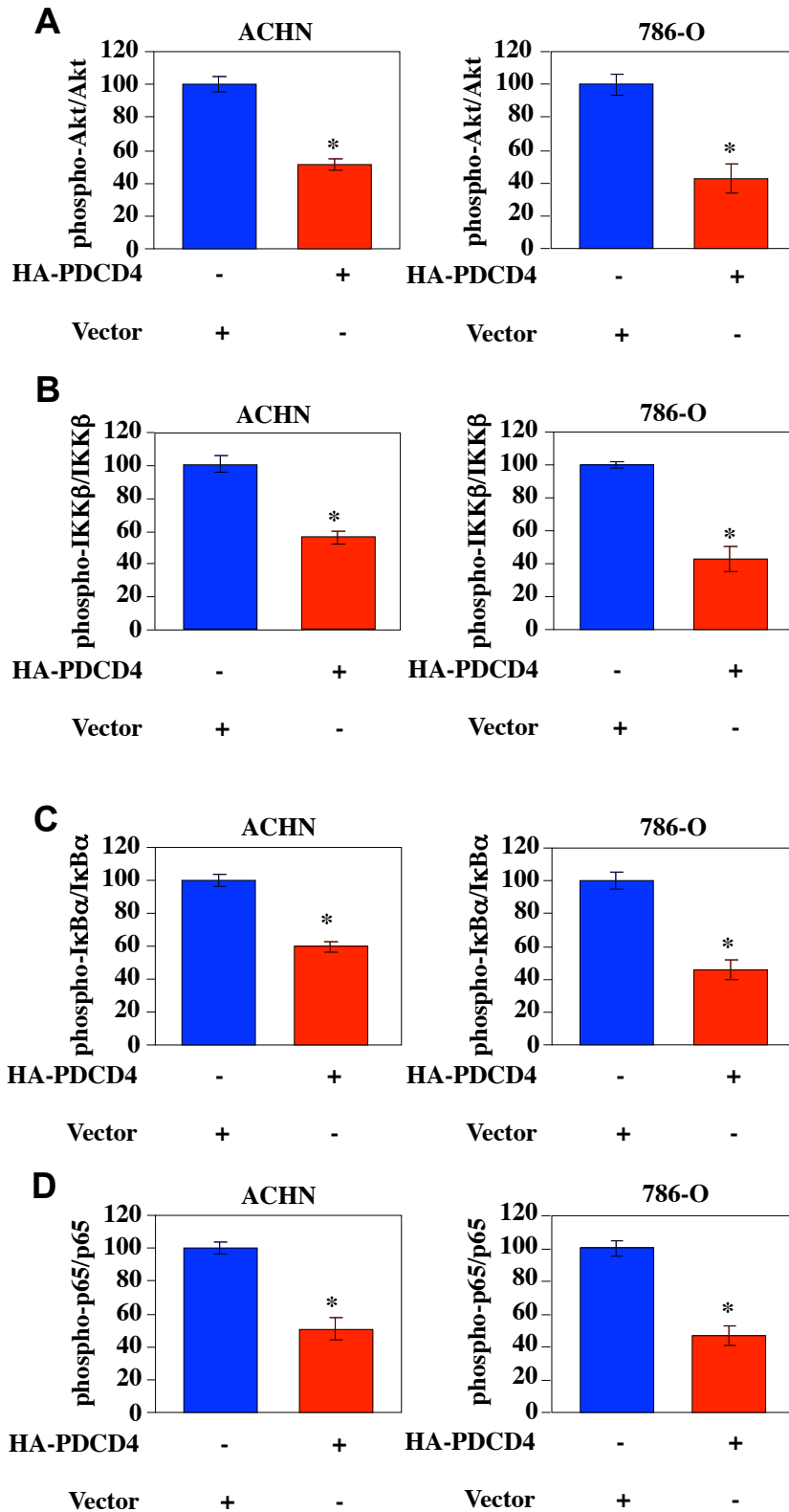
**Supplementary Fig. S1.**(A) Quantification of the results shown in Fig. 1A. Ratio of PDCD4 to actin is plotted. Mean  $\pm$  SE of 3 independent experiments is shown. \* $p < 0.01$  vs HK2. (B) Expression of miR-21 inhibits PDCD4 3'UTR-Luc. ACHN and 786-O renal cancer cells were transfected with the CMV-miR-21 expression vector and a reporter plasmid in which PDCD4 3' UTR is fused downstream of firefly luciferase cDNA. Luciferase activity was determined as described in the Materials and Methods. Mean  $\pm$  SE of 5 measurements is shown. \* $p = 0.001$  vs vector control. Bottom panels show expression of miR-21 from transfected vectors. (C) Expression of miR-21 Sponge as indicated by GFP mRNA expression for Fig. 1B.



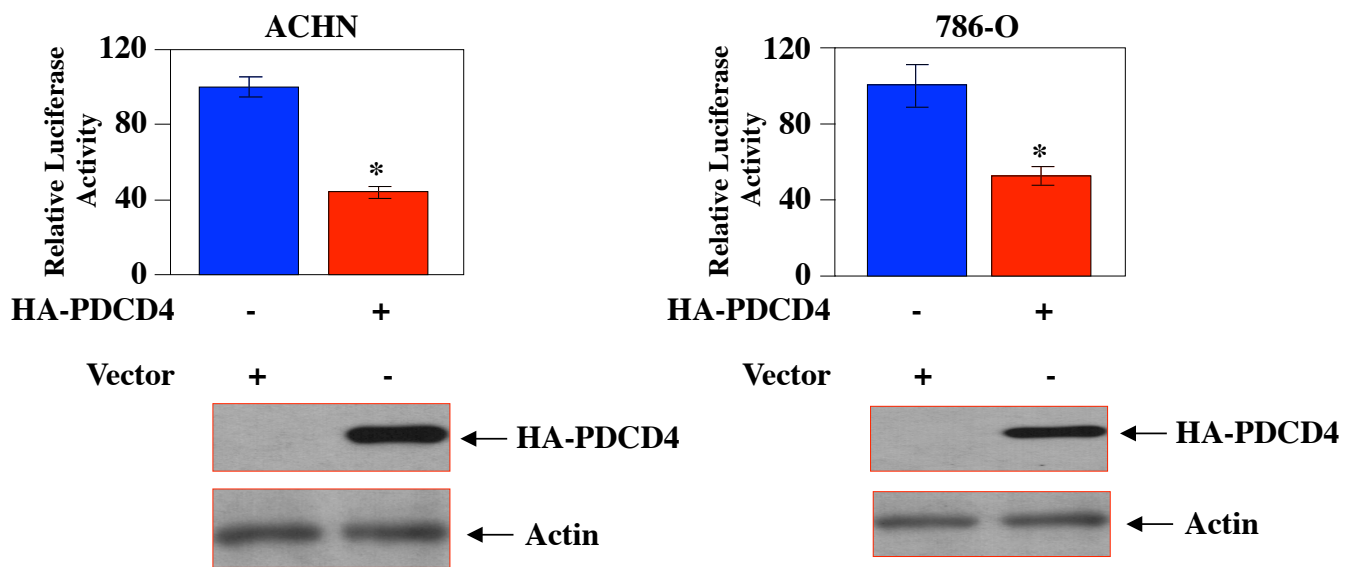
**Supplementary Fig. S1.** (D) Quantification of the results shown in Fig. 1C. Ratio of PDCD4 to actin is plotted. Mean  $\pm$  SE of 3 independent experiments is shown. \* $p = 0.0003$  vs vector. Expression of miR-21 Sponge for this panel is shown at the bottom. Expression of GAPDH mRNA was used as loading control.



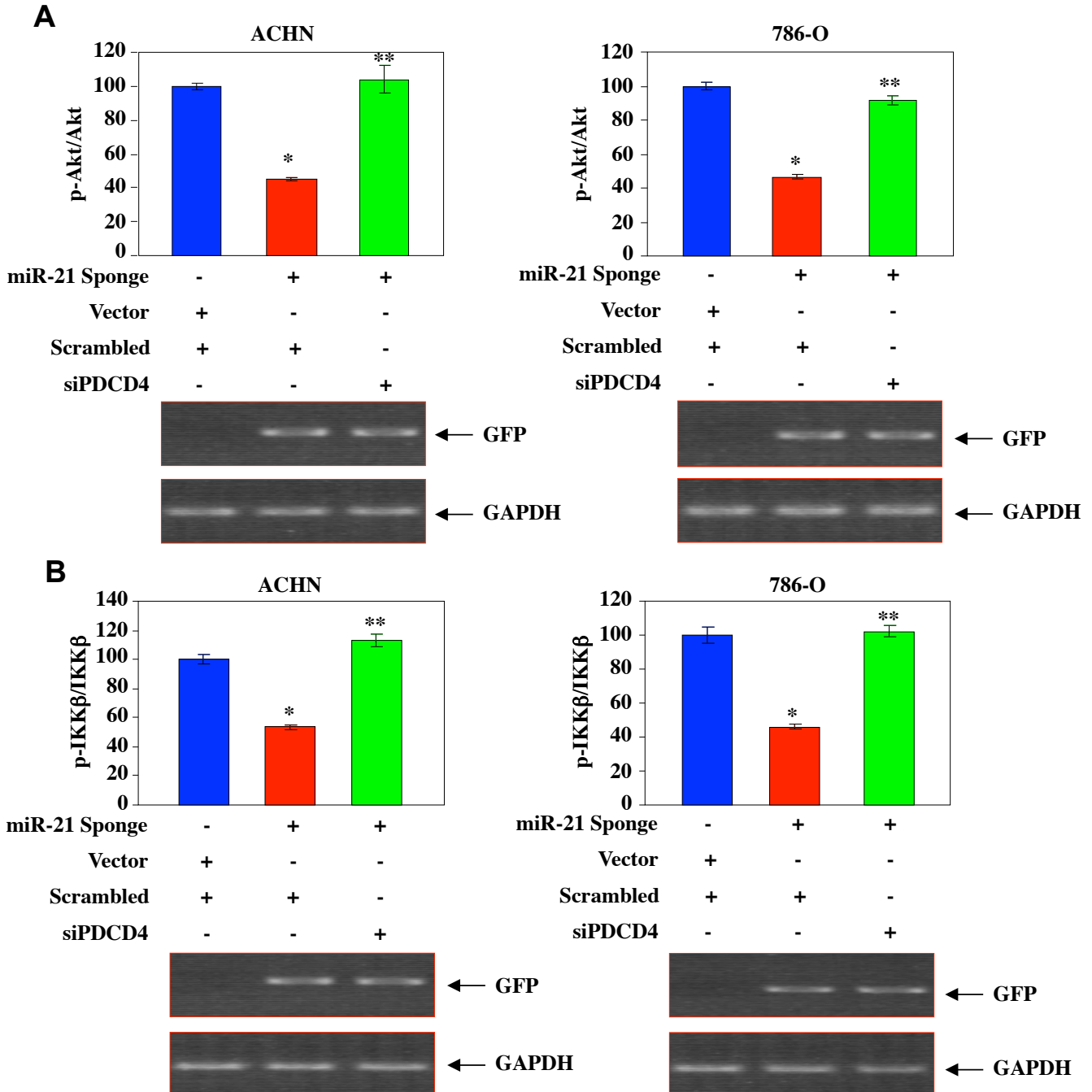
**Supplementary Fig. S2.** (A) Quantification of migration shown in Fig. 1D. The stains from the filter papers in the migration chambers were eluted and the absorbance was determined as a measure of number of cells as described in the Methods. Mean  $\pm$  SE of triplicate membranes is shown. \* $p < 0.001$  vs Vector; \*\* $p < 0.001$  vs miR-21 Sponge alone. Bottom parts show expression of miR-21. Expression of GFP mRNA was used as indicator of miR-21. GAPDH expression was used as control. Also, expression of PDCD4 protein is shown in parallel samples. Level of actin is shown as control. (B) Quantification of invasion shown in Fig. 1E. The stains were eluted as described above. Mean  $\pm$  SE of triplicate membranes is shown. \* $p < 0.001$  vs Vector; \*\* $p < 0.001$  vs miR-21 Sponge alone. Bottom parts show expression of GFP mRNA as indicator of miR-21 Sponge expression. Expression of GFP and GAPDH was determined by RT-PCR from total RNAs prepared from parallel samples. Also, expression of PDCD4 protein is shown in parallel samples.



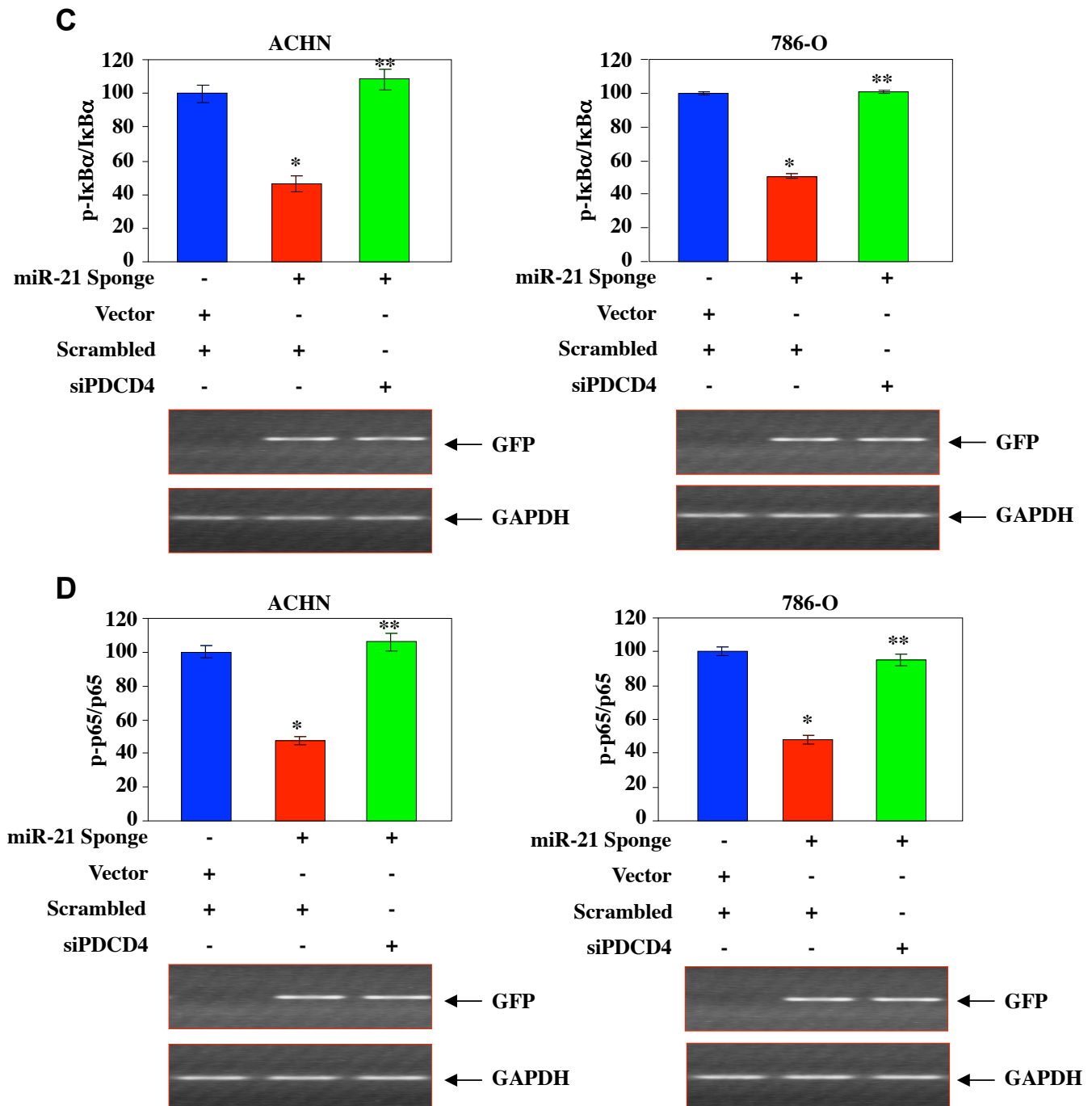
**Supplementary Fig. 3.** (A) Quantification of the results shown in Fig. 2. Ratio of phospho-Akt (Ser-473) to Akt (panel A), phospho-IKK $\beta$  to IKK $\beta$  (panel B), phospho-I $\kappa$ B $\alpha$  to I $\kappa$ B $\alpha$  (panel C) and phospho-p65 (Ser-536) to p65 (panel D) is plotted. Mean  $\pm$  SE of 4 independent experiments is shown. \* $p < 0.0002$  vs vector.



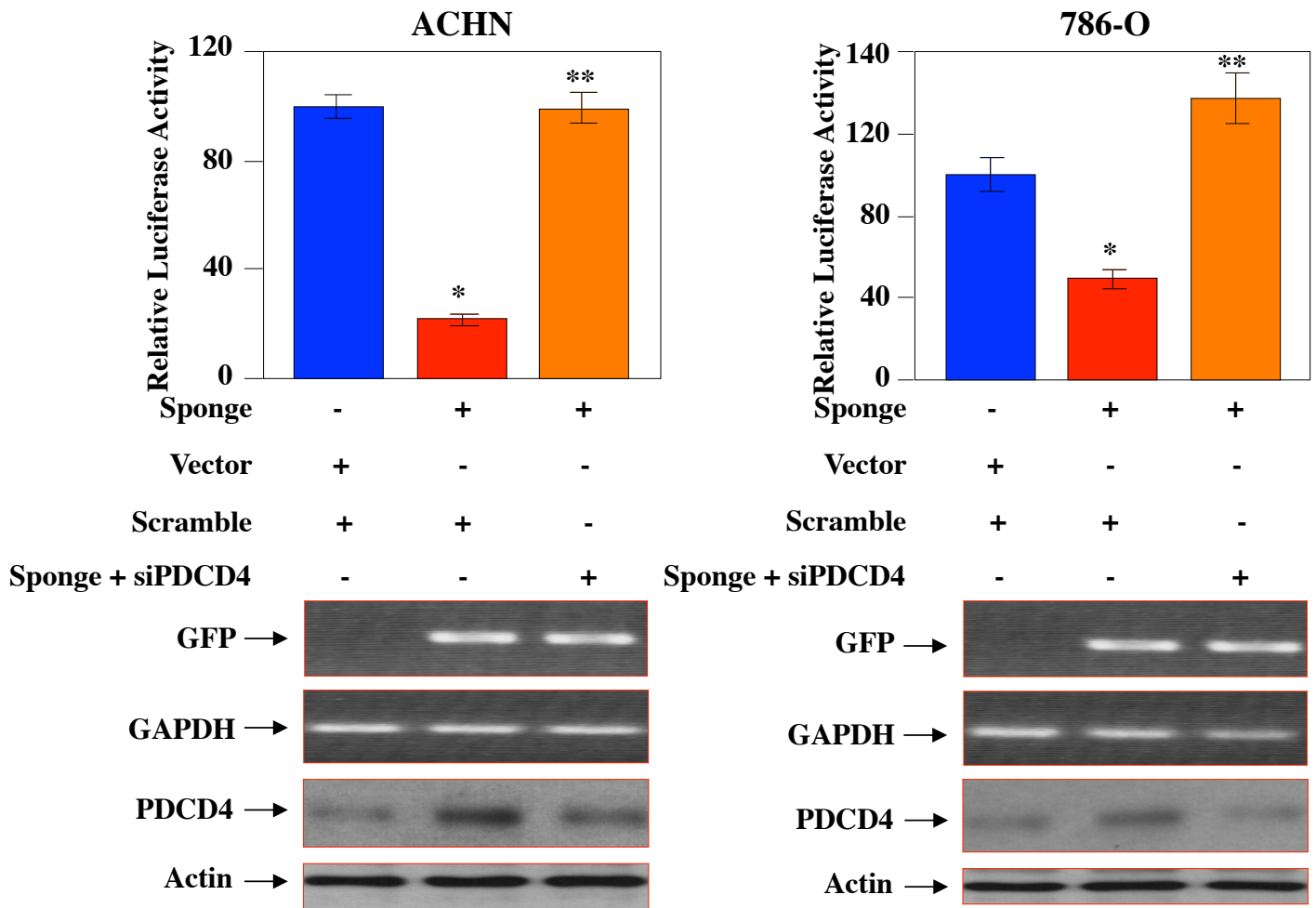
**Supplementary Fig. S4.** PDCD4 inhibits NFκB-dependent transcription in ACHN and 786-O cells. ACHN and 786-O renal carcinoma cells were transfected with NFκB-Luc reporter construct along with HA- tagged PDCD4 expression vector as indicated. The luciferase activity was determined as described in the Materials and Methods. Mean  $\pm$  SE of six measurements is shown. Relative luciferase activity is shown. \*p = 0.001vs vector control. Bottom panels show expression of HA-tagged PDCD4 and actin in parallel samples.



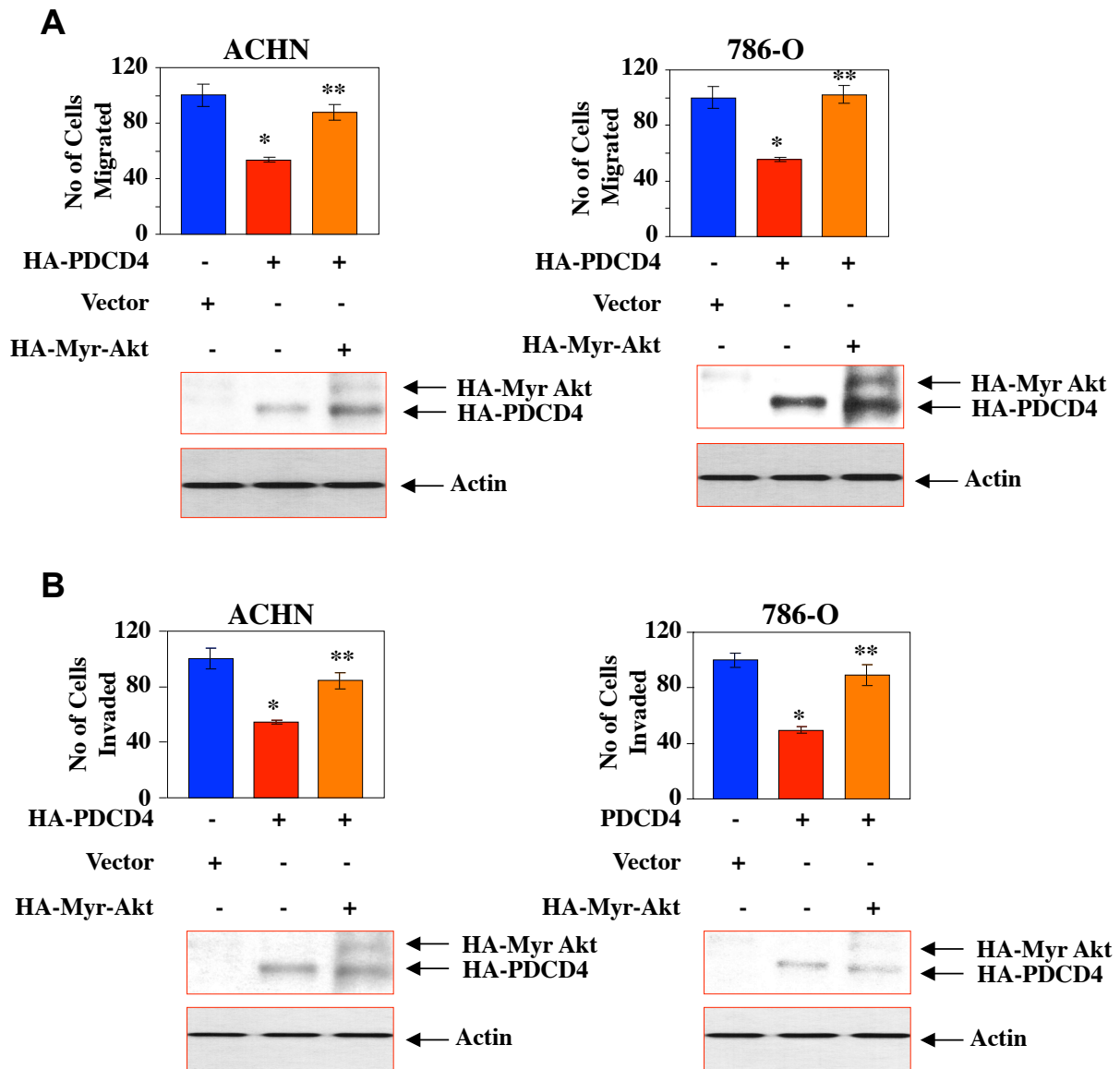
**Supplementary Fig. S5.** Quantification of the results shown in Fig. 3A and 3B. Ratio of phospho-Akt (Ser-473) to Akt (panel A) and phospho-IKK $\beta$  to IKK $\beta$  (panel B) is shown. Mean  $\pm$  SE of 3 independent experiments is shown. \* $p < 0.01$  vs vector. \*\* $p < 0.01$  vs Sponge. Expression of miR-21 Sponge as indicated by GFP mRNA expression for these panels is shown. Expression of GFP and GAPDH was determined by RT-PCR from total RNAs prepared from parallel samples used in Fig. 3A and Fig. 3B respectively.



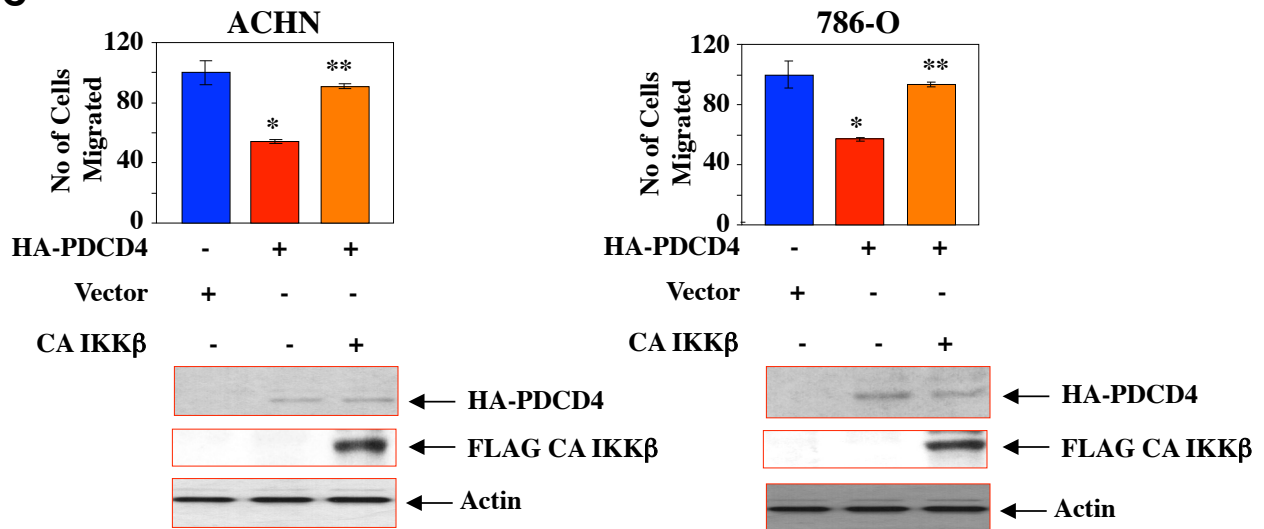
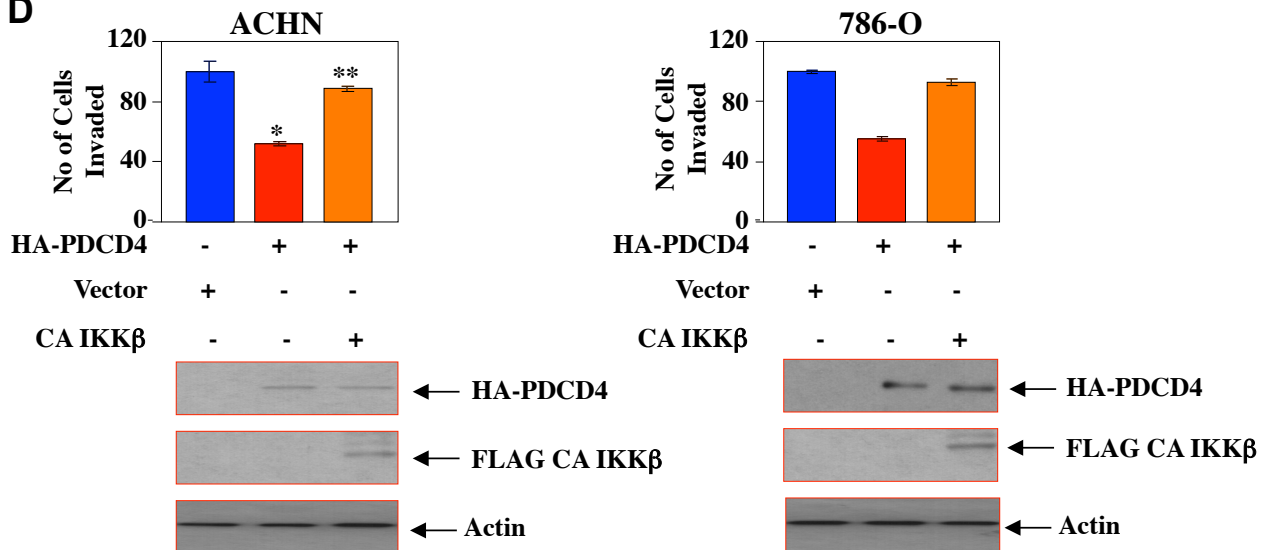
**Supplementary Fig. S5.** Quantification of the results shown in Fig. 3C and 3D. Ratio of phospho-IκBα to IκBα (panel C) and phospho-p65 to p65 (panel D) is shown. Mean ± SE of 3 independent experiments is shown. \*p < 0.01 vs vector. \*\*p < 0.01 vs Sponge. Expression of miR-21 Sponge as indicated by GFP mRNA expression for these panels is shown. Expression of GFP and GAPDH was determined by RT-PCR from total RNAs prepared from parallel samples used in Fig. 3C and Fig. 3D respectively.



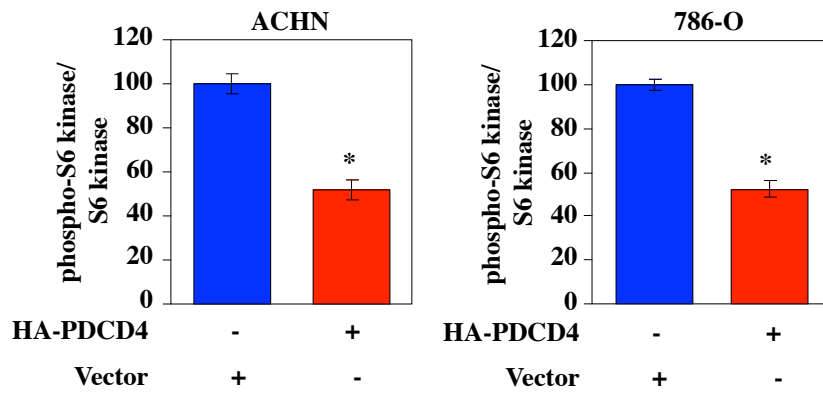
**Supplementary Fig. S6.** miR-21-target PDCD4 regulates NFκB-dependent reporter transcription. NFκB-Luc reporter plasmid was cotransfected with miR-21 Sponge and siRNAs against PDCD4 into ACHN and 786-O renal cancer cells as described in the Materials and Methods. The luciferase activity was determined. Mean ± SE of 6 measurements is shown. \*p < 0.001 vs control; \*\*p < 0.001 vs miR-21Sponge alone. Relative luciferase activity is shown. GFP mRNA as indicator of miR-21 Sponge expression is shown in parallel samples of same experiment. Expression of GAPDH mRNA was used as loading control. Also, expression of PDCD4 protein is shown in the lysates. Expression of actin was used as loading control.



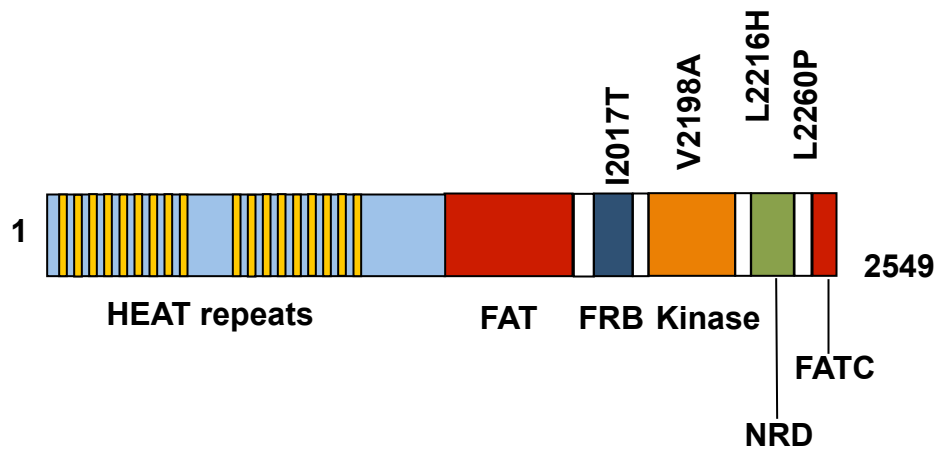
**Supplementary Fig. S7A and S7B.** Quantification of migration and invasion of ACHN and 786-O renal cancer cells shown in Figs. 4A and 4B. (A) The stains from the filter papers in the migration chambers described in Figs. 4A and 4B were eluted and the absorbance was determined as a measure of number of cells as described in the Materials and Methods. Mean  $\pm$  SE of triplicate membranes is shown. \* $p < 0.001$  vs Vector; \*\* $p < 0.001$  vs PDCD4. Bottom panel shows expression of HA-tagged Myr Akt and PDCD4. Expression of actin was used as loading control.

**C****D**

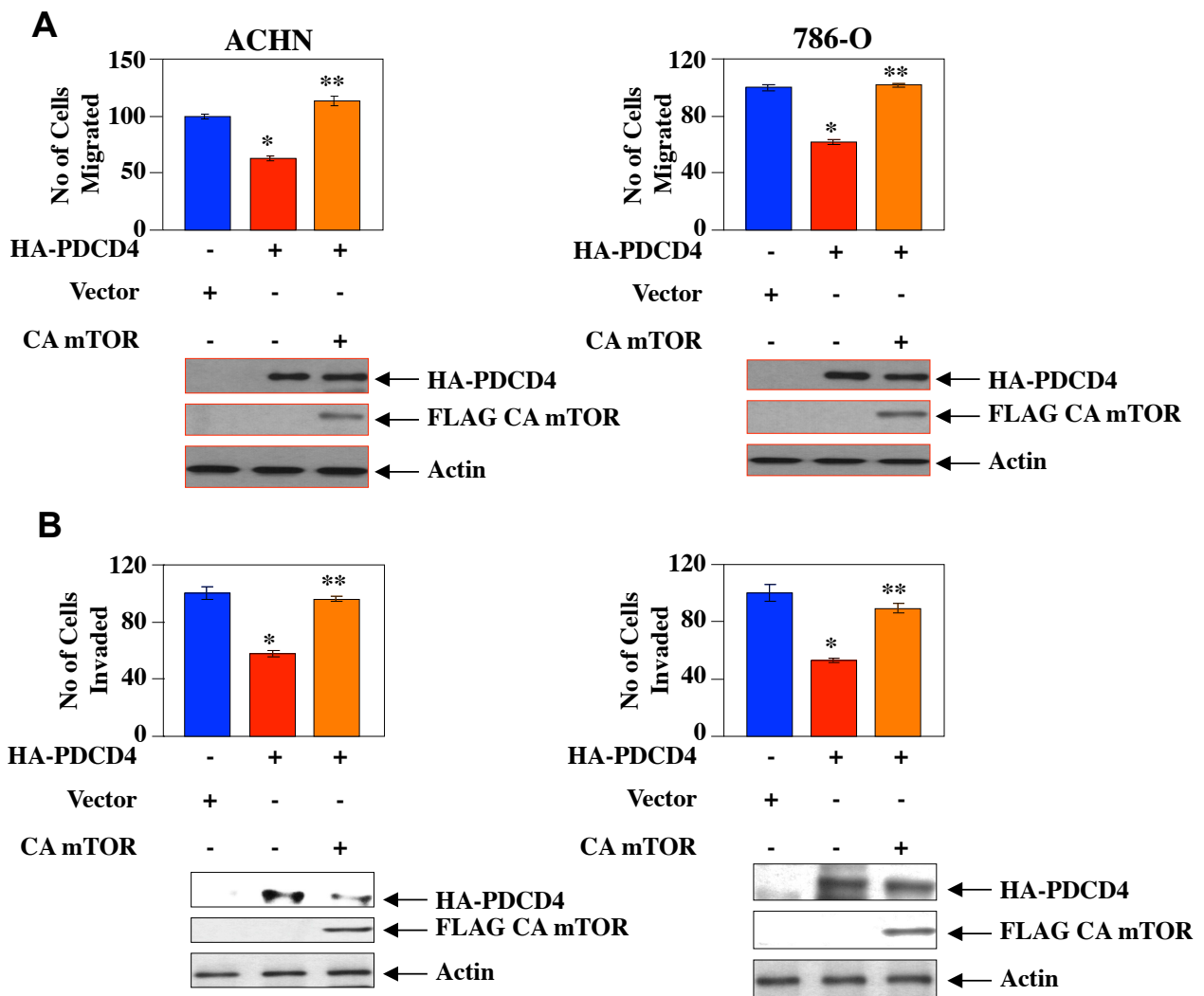
**Supplementary Fig. S7C and S7D.** Quantification of migration and invasion of ACHN and 786-O renal cancer cells shown in Figs. 4C and 4D. The stains from the filter papers in the migration chambers described in Figs. 4C and 4D were eluted and the absorbance was determined as a measure of number of cells as described in the Materials and Methods. Mean  $\pm$  SE of triplicate membranes is shown. \* $p < 0.001$  vs Vector; \*\* $p < 0.001$  vs PDCD4. Bottom panel shows expression of HA-tagged CA IKK $\beta$  and PDCD4. Expression of actin was used as loading control.



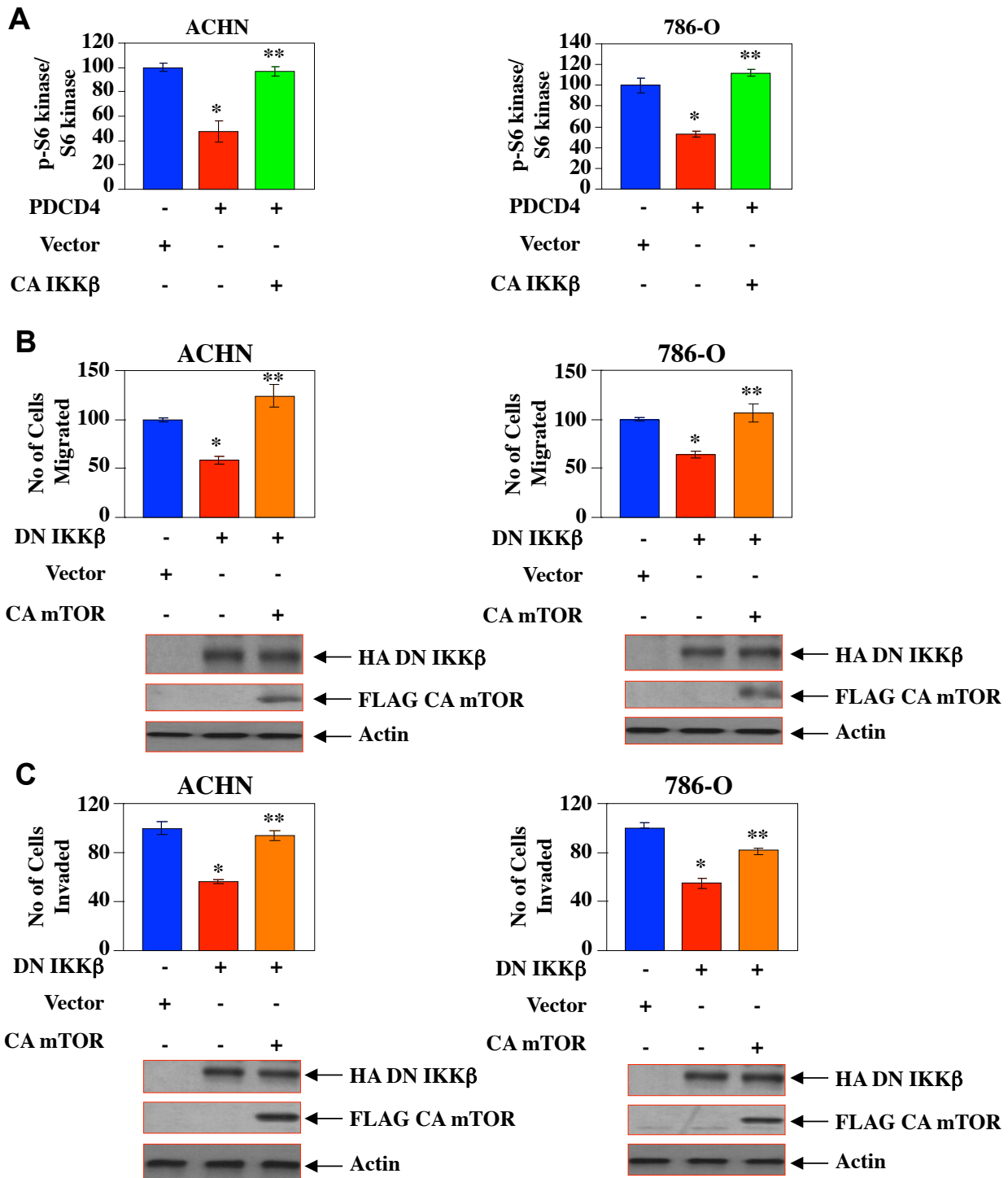
**Supplementary Fig. S8.** Quantification of the results shown in Fig. 5A. Ratio of phospho-S6 kinase (Thr-389) to S6 kinase is shown. Mean  $\pm$  SE of 4 independent experiments is shown. \*p = 0.0008 vs vector.



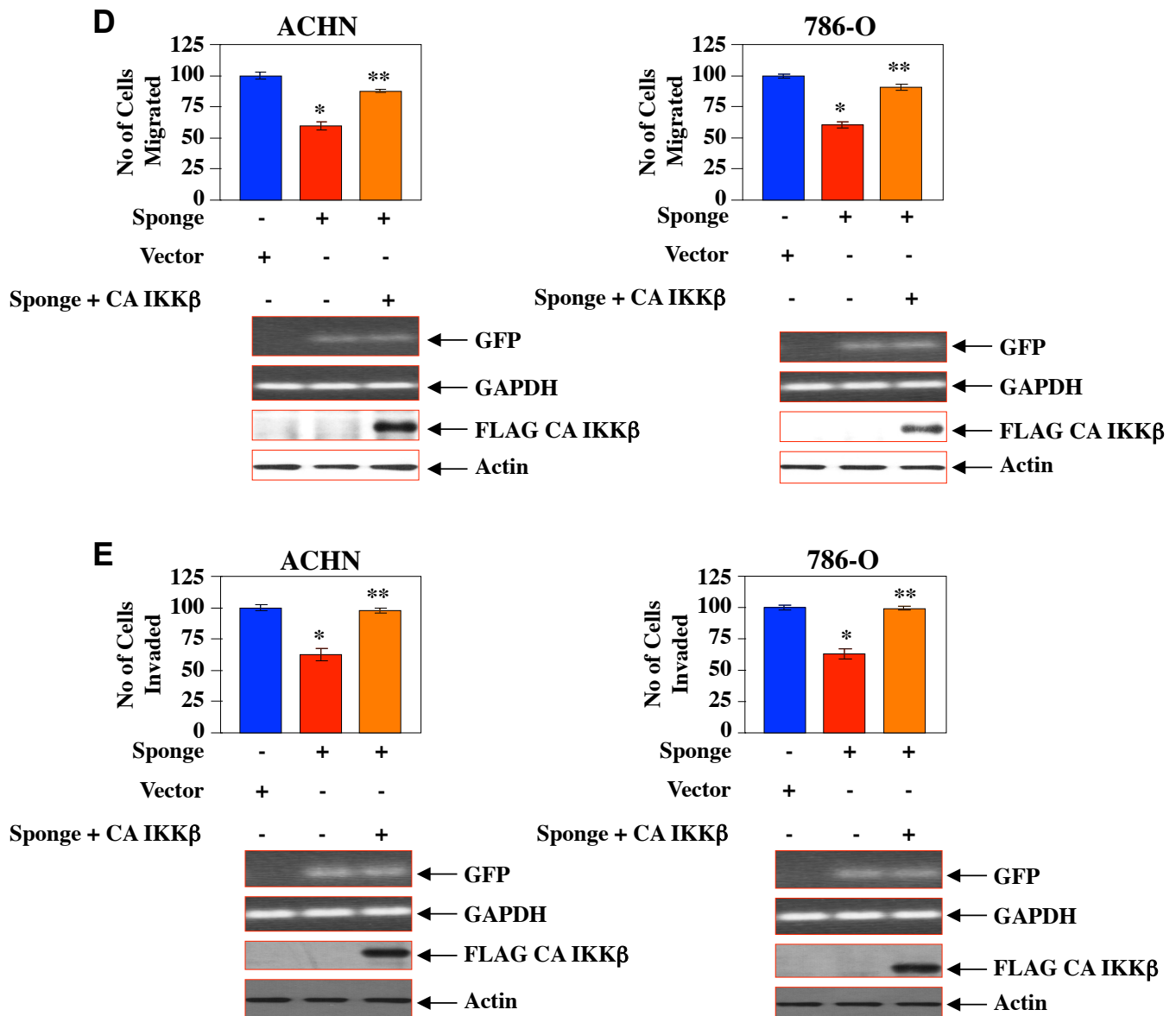
**Supplementary Fig S9.** Structure of the constitutively active mutant of mTOR, which acts as mTORC1. The changes in amino acid are shown at the top. The protein domains are shown at the bottom. HEAT = Huntington, EF3, A subunit of PP2A, TOR1; FAT = FRAP, ATM, TRAP; FRB = FKBP12-Rapamycin Binding; NRD = Negative Regulatory Domain. FATC = FAT c-terminal domain.



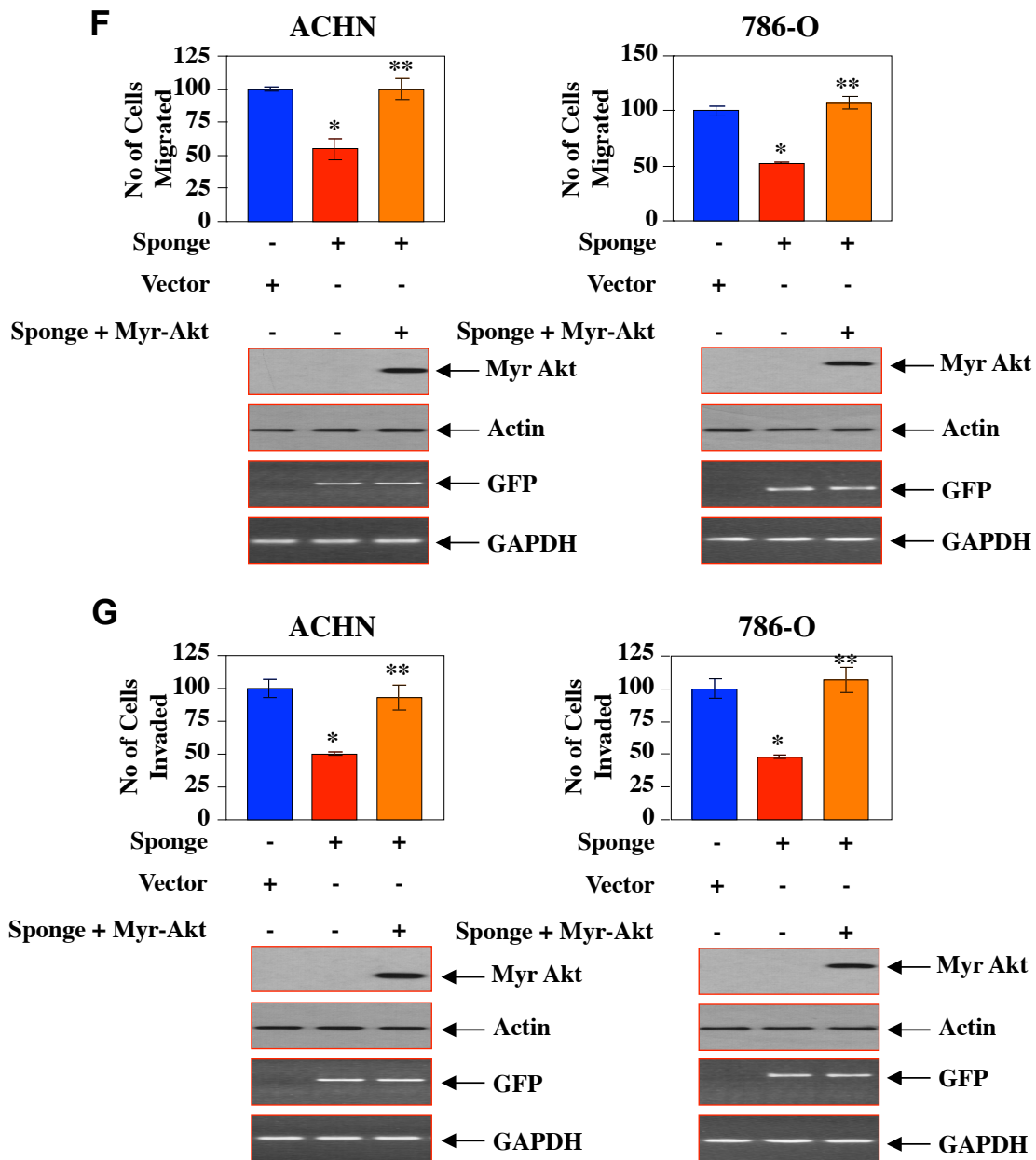
**Supplementary Fig. S10A and S10B.** Quantification of migration and invasion of ACHN and 786-O renal cancer cells shown in Figs. 5B and 5C. (A) The stains from the filter papers in the migration chambers described in Figs. 5B and 5C were eluted and the absorbance was determined as a measure of number of cells as described in the Materials and Methods. Mean  $\pm$  SE of triplicate membranes is shown. \* $p < 0.001$  vs Vector; \*\* $p < 0.001$  vs PDCD4. Bottom panel shows expression of HA-tagged PDCD4 and FLAG-tagged mTOR. Expression of actin was used as loading control.



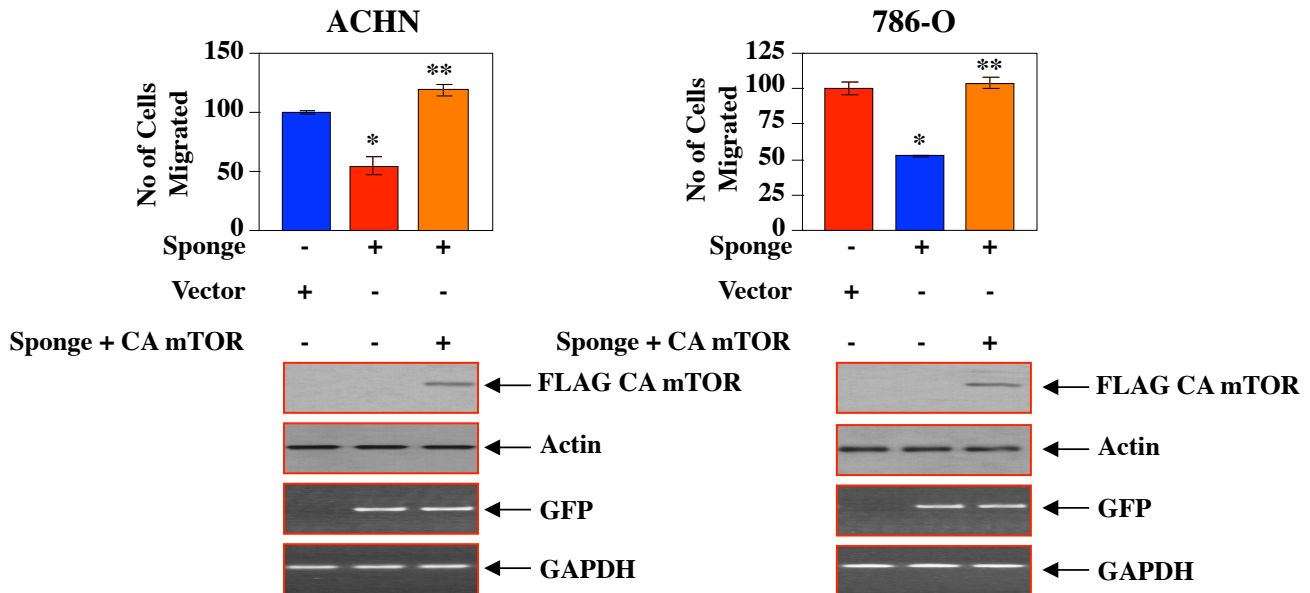
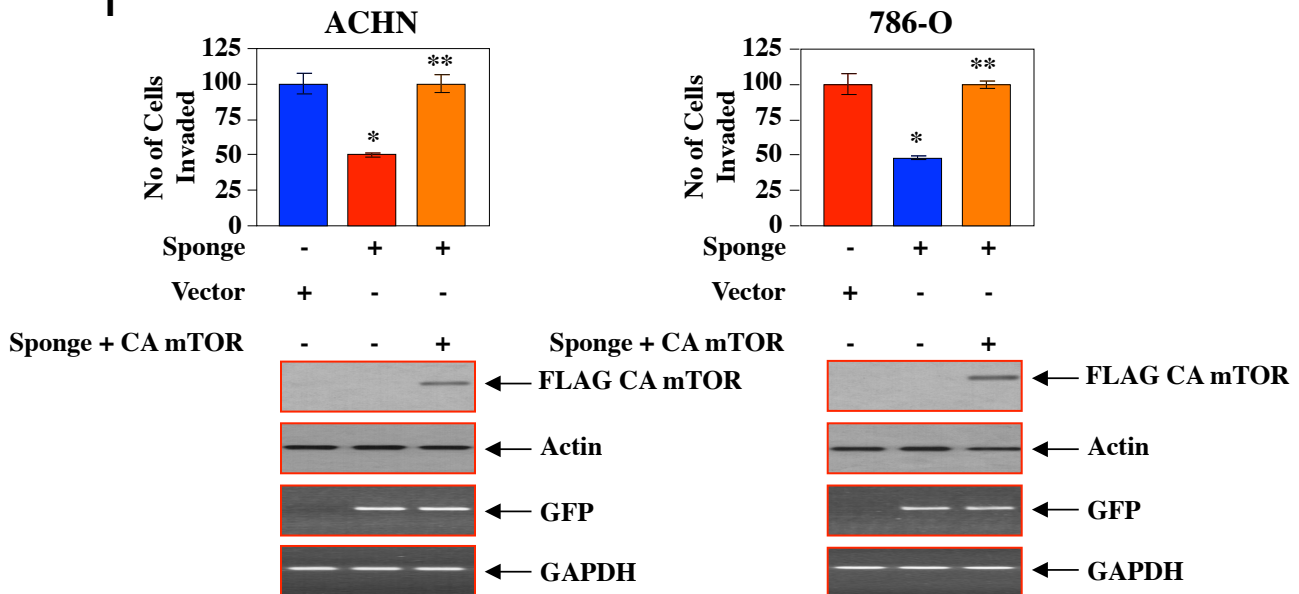
**Supplementary Fig. 11A, 11B and 11C.** Quantification of the results shown in Fig. 6A. Ratio of phospho-S6 kinase (Thr-389) to S6 kinase (panel A) is shown. Mean  $\pm$  SE of 3 independent experiments is shown. \* $p < 0.01$  vs vector; \*\* $p < 0.01$  vs PDCD4. Quantification of migration (panel B) and invasion (panel C) of ACHN and 786-O renal cancer cells shown in Figs. 6B and 6C. The stains from the filter papers in the migration chambers described in Figs. 6B and 6C were eluted and the absorbance was determined as a measure of number of cells as described in the Materials and Methods. Mean  $\pm$  SE of triplicate membranes is shown. \* $p < 0.001$  vs Vector; \*\* $p < 0.001$  vs DN IKK $\beta$ . Bottom panel shows expression of HA-tagged DN IKK $\beta$  and FLAG-tagged DN mTOR. Expression of actin was used as loading control.



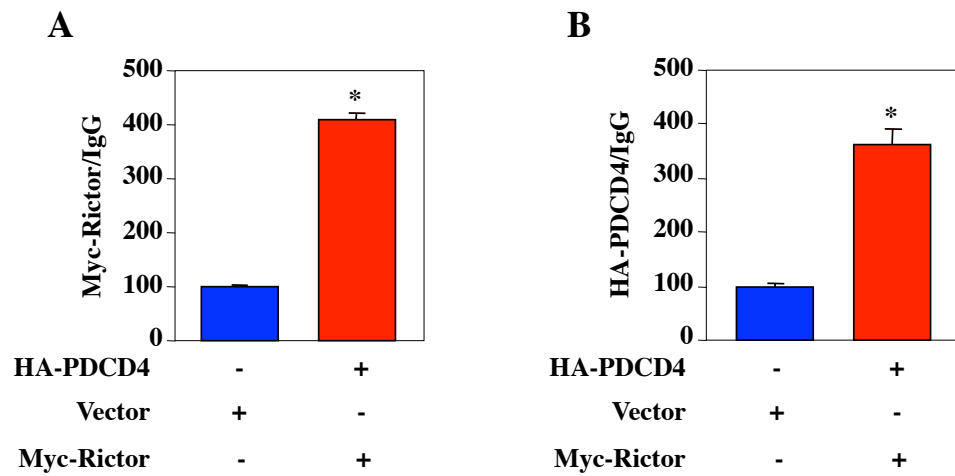
**Supplementary Fig. S11D and S11E.** Quantification of migration (panel D) and invasion (panel E) of ACHN and 786-O renal cancer cells shown in Figs. 6D and 6E. The stains from the filter papers in the migration chambers described in Figs. 6D and 6E were eluted and the absorbance was determined as a measure of number of cells as described in the Materials and Methods. Mean  $\pm$  SE of triplicate membranes is shown. \* $p < 0.001$  vs Vector; \*\* $p < 0.001$  vs mir-21 Sponge. Bottom panels show expression of GFP as a surrogate of miR-21 Sponge expression. Also, expression of FLAG-tagged CA IKK $\beta$  is shown. Expression of actin was used as loading control.



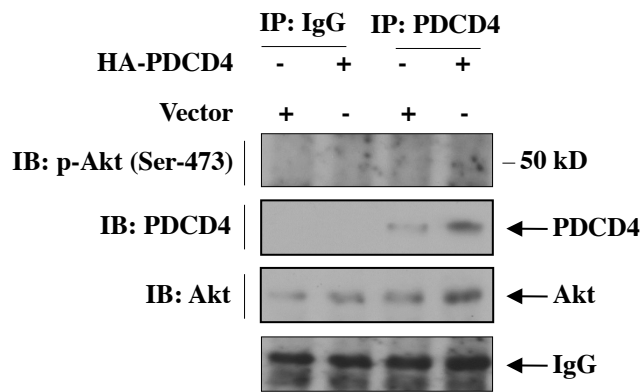
**Supplementary Fig. S11F and S11G.** Quantification of migration (F) and invasion (panel G) of ACHN and 786-O renal cancer cells shown in Figs. 6F and 6G. The stains from the filter papers in the chambers described in Figs. 6F and 6G were eluted and the absorbance was determined as a measure of number of cells as described in the Materials and Methods. Mean  $\pm$  SE of triplicate membranes is shown. \* $p < 0.001$  vs Vector; \*\* $p < 0.001$  vs miR-21 Sponge. Bottom panels show expression of GFP as a surrogate of miR-21 Sponge expression. Also, expression of HA-tagged Myr-Akt is shown. Expression of actin was used as loading control.

**H****I**

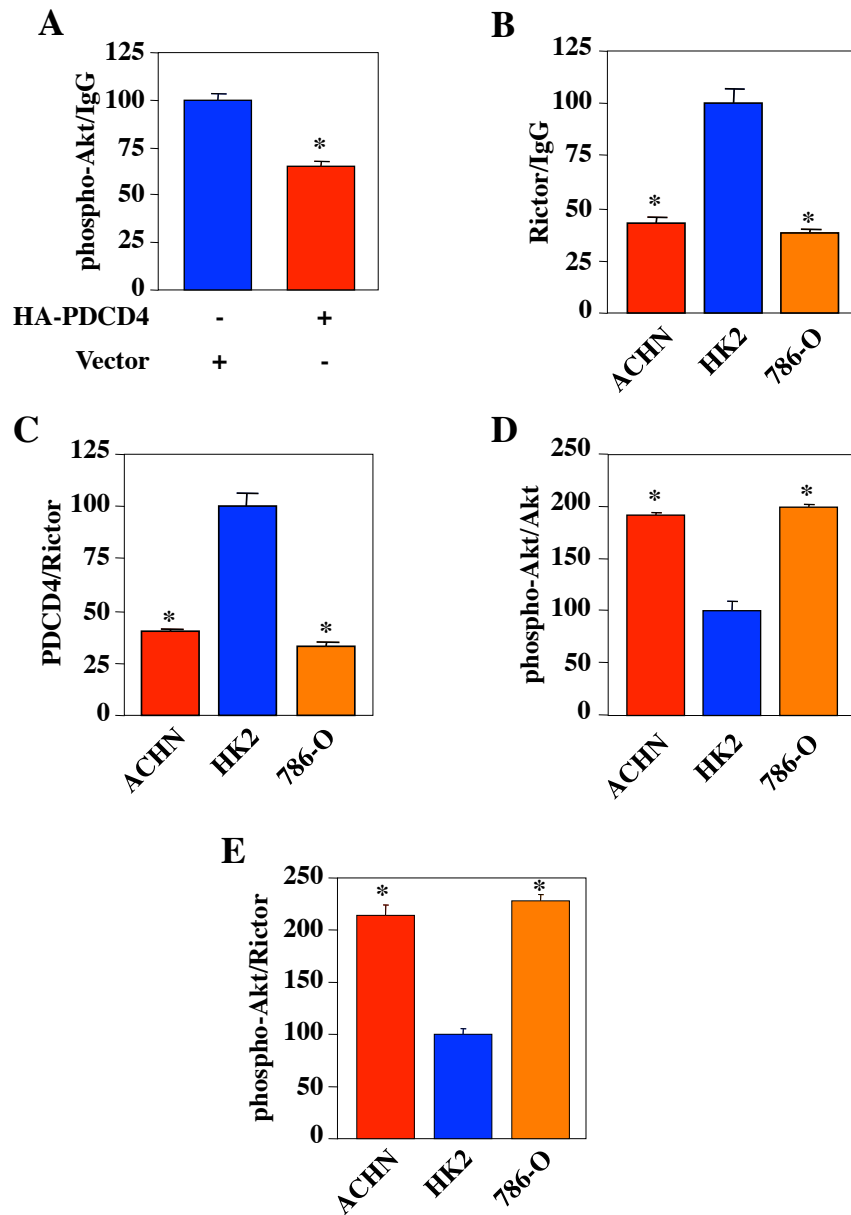
**Supplementary Fig. S11H and S11I.** Quantification of migration (panel H) and invasion (panel I) of ACHN and 786-O renal cancer cells shown in Figs. 6H and 6I. The stains from the filter papers in the chambers described in Figs. 6H and 6I were eluted and the absorbance was determined as a measure of number of cells as described in the Materials and Methods. Mean  $\pm$  SE of triplicate membranes is shown. \* $p < 0.001$  vs Vector; \*\* $p < 0.001$  vs miR-21 Sponge. Bottom panels show expression of GFP as a surrogate of miR-21 Sponge expression. Also, expression of FLAG-tagged CA mTOR is shown. Expression of actin was used as loading control.



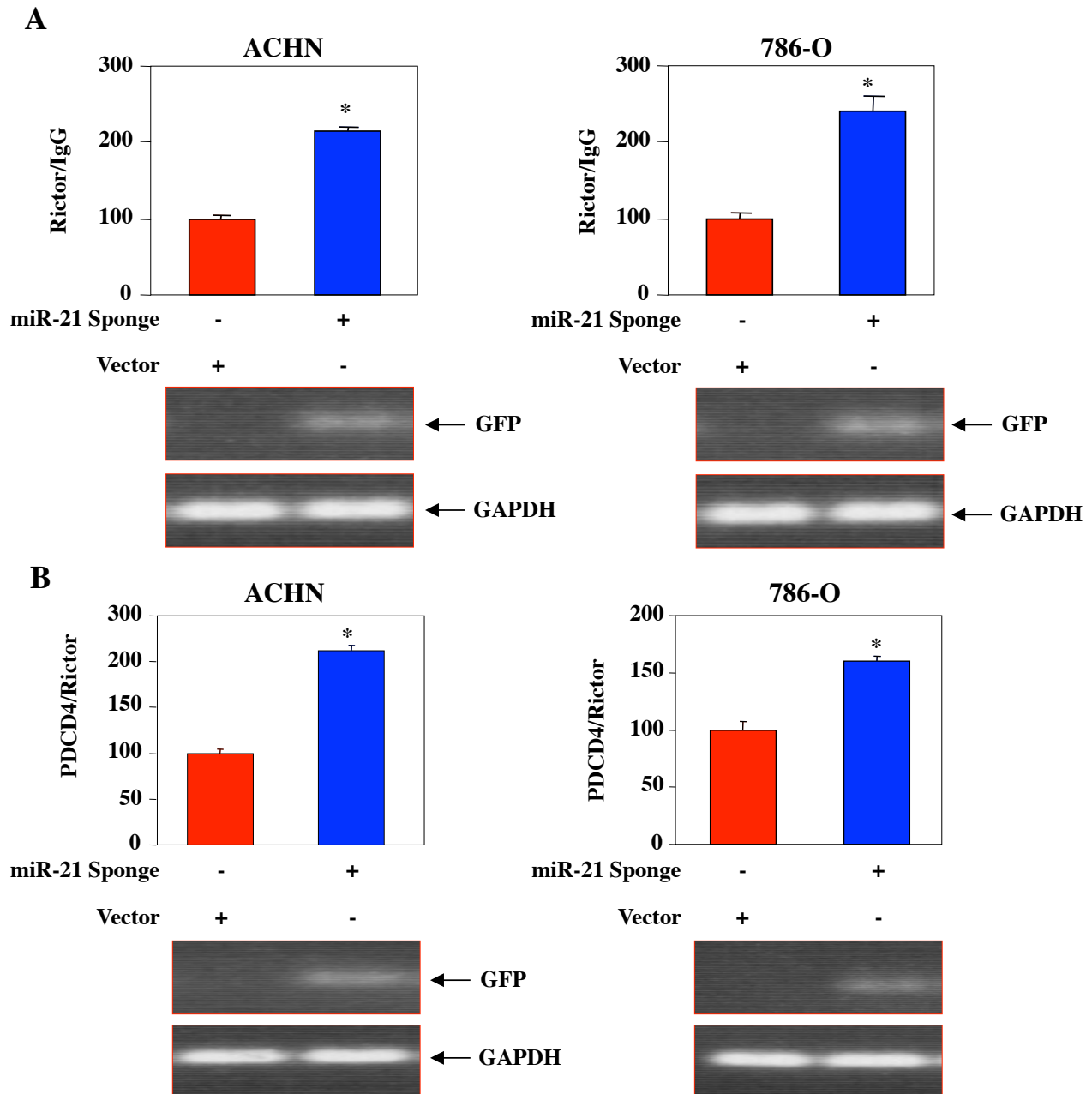
**Supplementary Fig. S12A and S12B.** Quantification of the results shown in Figs. 7A and 7B. Ratio of Myc-Rictor to IgG (panel A) and HA-PDCD4 to IgG (panel B) is plotted. Mean  $\pm$  SE of 4 independent experiments is shown. \* $p = 0.001$  vs vector in panel A, and 0.0024 for panel B.



**Supplementary Fig. S13.** Measurement of mTORC2 activity in the PDCD4 immunoprecipitates. HK2 cells were transfected with HA-tagged PDCD4 or vector. The cell lysates were immunoprecipitated with IgG or PDCD4 antibody. The immunoprecipitates were used for immunocomplex kinase assay using 100 ng of recombinant inactive Akt as substrate. Note that no phosphorylation of Akt at Ser-473 was detected. For Akt blot 5 times less of input recombinant Akt (20 ng) was used.



**Supplementary Fig. S14.** (A) Quantification of results shown in Fig. 7C. Ratio of phospho-Akt (Ser-473) to IgG is plotted. Mean  $\pm$  SE of 5 independent experiments is shown. \* $p = 0.0002$  vs vector. (B) Quantification of the results shown in Fig. 7D. Since expression of PDCD4 is regulated between normal proximal tubular epithelial cells and renal cancer cells, ratio of rictor to IgG is plotted. Mean  $\pm$  SE of 4 independent experiments is shown. \* $p < 0.0001$  vs HK2 cells. (C) Quantification of the results shown in Fig. 7E. Ratio of PDCD4 to rictor is plotted. Mean  $\pm$  SE of 3 independent experiments is shown. \* $p < 0.0001$  vs HK2 cells. (D) Quantification of the results shown in Fig. 7F. Ratio of phospho-Akt (Ser-473) to Akt is plotted. Mean  $\pm$  SE of 6 independent experiments is shown. \* $p < 0.001$  vs HK2 cells. (E) Quantification of the results shown in Fig. 7G. Ratio of phospho-Akt to rictor is shown. Mean  $\pm$  SE of 4 independent experiments is shown. \* $p < 0.0001$  vs HK2 cells.



**Supplementary Fig. 15A.** Quantification of the results shown in Fig. 8A and 8B. (A) Ratio of rictor to IgG from Fig. 8A is plotted. Mean  $\pm$  SE of 3 experiments is shown. \* $p = 0.0043$  vs vector for left panel and  $0.009$  vs vector for right panel. (B) Ratio of PDCD4 to rictor from Fig. 8B is plotted. Mean  $\pm$  SE of 4 experiments is shown. \* $p = 0.0001$  vs vector for left panel and  $0.007$  vs vector for right panel. Expression of GFP as a surrogate of miR-21 Sponge expression with GAPDH is shown for Fig. 8A and 8B.